First-principles study of the energy-gap composition dependence of $Zn_{1-x}Be_xSe$ ternary alloys

A. Berghout,[1,2] A. Zaoui,[2,*] J. Hugel,[1] and M. Ferhat[3]
[1]*LPMD, Institut de Physique Electronique et de Chimie, 1 Boulevard, Dominique François Arago, CP 87811, 57078 Metz Cedex 3, France*
[2]*LML, Ecole Polytechnique de Lille, Université des Sciences et Technologie de Lille, Cité Scientifique, Avenue Paul Langevin, 59655 Villeneuve d'Ascq Cedex, France*
[3]*Département de Physique, Université des Sciences et de la Technologie d'Oran, 31000 Oran, Algeria*
(Received 6 October 2006; revised manuscript received 1 March 2007; published 15 May 2007)

We report the results of a self-consistent pseudopotential study including structural, optical, and thermodynamic properties of cubic $Zn_{1-x}Be_xSe$ semiconductor alloy. The system is modeled in various possible configurations using a large 64-atom supercell. The evaluated band-gap bowing is in good agreement with the experimental data. The different roles of structural and chemical effects on the gap bowing and its variation with composition are identified and discussed. It is found that structural effect, i.e., the relaxation of atomic bonds, overwhelms the other contributions to the gap bowing. Lattice parameter fulfills Vegard's law with a small downward bowing deviation of about 0.04 Å. Our calculated bond lengths appear to be more reliable compared with those obtained from previous theoretical studies using smaller atomic supercell. Besides, a regular-solution model was used to investigate the thermodynamic stability of $Zn_{1-x}Be_xSe$, which mainly indicates a wide phase miscibility gap.

DOI: 10.1103/PhysRevB.75.205112 PACS number(s): 73.43.Cd, 73.61.Ey, 74.25.Bt, 74.25.Jb

I. INTRODUCTION

Alloys represent important classes of materials ranging from metallic alloys, where mechanical and magnetic properties can be controlled, to semiconductors, where delicate electronic properties are tuned by composition. The possibility to alloy semiconductors in order to tune the band-gap energy according to the device's applications has attracted a great deal of attention from both the experimental and theoretical points of view. Recent years[1–7] have seen great progress in the development of epitaxial growth techniques, which leads to successful synthesis of alloys of distinctly different semiconductor materials. A special attention was paid to the wide-band-gap semiconductors category and their different optoelectronic applications such as light-emitting diodes and laser diodes. ZnSe is one of the promising material systems due to the fact that efficient light emission at short wavelengths (green and blue regions of the visible spectrum) can be realized. However, device degradation occurring in ZnSe-based structures (ZnSSe, ZnMgSSe, etc.) has been found to be a compromising problem with these structures. To overcome this shortcoming, beryllium chalcogenides, characterized by their higher degree of covalent bonding as compared to other more ionic wide-gap II-VI semiconductors such as ZnSe, were proposed as new candidates to increase the resistance of the structures to dislocations, point defects, and their propagation in order to extend the lifetime and efficiency of these devices by increasing the bond strength of the II-VI materials involved.[1,2]

$Zn_{1-x}Be_xSe$, which is a real example of alloying binary compounds with contrasted physical properties, interested more and more scientific community.[2–7] The substitution of Zn by Be is accompanied by the decrease of the lattice parameter and a simultaneous rise in the energy band gap. Wilmers *et al.*[3] examined $Zn_{1-x}Be_xSe$ alloys throughout the 0–1 Be concentration range using vaccum ultraviolet ellipsometer, from which they determined the dielectric functions of this system. The reported x dependence of the band gap exhibited an important deviation from linearity (band-gap bowing value of 1.1 eV). More recently, Chauvet *et al.*[4] published the investigation of the band gap of the same system with x up to 0.70. The latest was determined from photoluminescence and reflectivity measurements. They reported a band-gap bowing value of 0.97 eV and determined the direct-to-indirect gap crossover at the composition $x=0.46$.

To model the alloy system, relatively small supercells were used; for instance 8-, 16-, and 32-atom supercells (see Refs. 8 and 9 for additional evidence). Tsai *et al.*[8] employed first-principles molecular dynamics combined with pseudofunction method to investigate the electronic and structural properties of $Zn_{1-x}Be_xSe$, $Zn_{1-x}Cd_xSe$, and $Zn_{1-x}Se_xTe$ using 8-atom supercells. Their results for $Zn_{1-x}Be_xSe$ underestimate the slope of the band gap and overestimated the value of the band-gap bowing, compared with the experimental ones. They attributed the behavior of the band gap in the region of $x \leqslant 0.5$ to the near constant values of bond lengths. Indeed, the Be-Se bond behavior they found in the composition range $0.25 \leqslant x \leqslant 0.75$ is doubtful. The use of such supercells describes the semiconductor alloy as an ordered structure which is unrealistic and then limits the accuracy of the results. To make this problem clear, a detailed *ab initio* self-consistent study of the $Zn_{1-x}Be_xSe$ system employing larger supercells is therefore necessary.

The present work aims to extend the study of the composition dependence of the energy band gap of $Zn_{1-x}Be_xSe$ semiconductor alloys and to investigate in detail the physical origin of the band-gap bowing b in these systems. In addition to the consideration of the electronic structure, we also develop a detailed investigation of the more important quantities characterizing the atomic structure and the phase stability of $Zn_{1-x}Be_xSe$ system, which are related to the bowing behavior. In the subsequent text, the computational details

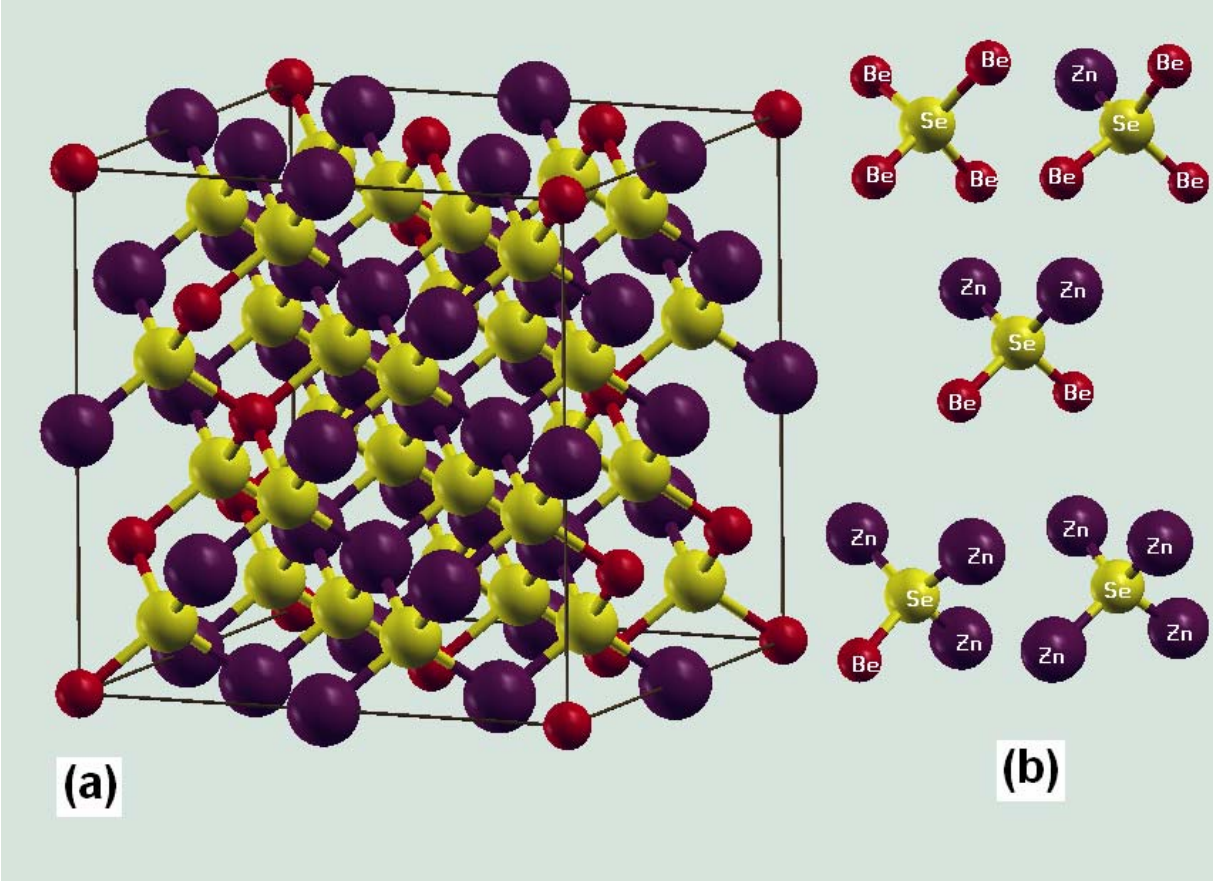

FIG. 1. (Color online) Representative 64-atom supercell treating $Zn_{24}Be_8Se_{32}$ semiconductor alloy used in the calculations (a). The five possible Se environment configurations are displayed in (b).

are given in Sec. II. The results are presented and discussed in Sec. III. Section IV is the conclusion.

II. COMPUTATIONAL DETAILS

The calculation was based on first-principles density-functional theory (DFT) with the local-density approximation (LDA),[10] as implemented in the plane-wave pseudopotential scheme.[11] The Ceperley-Alder electron-gas results[12] as interpolated by Perdew and Zunger[13] were used for the exchange-correlation potential. Pseudopotentials used in the present work are norm conserving[14,15] and were generated using scalar relativistic calculations. The Zn $3d$ electrons were treated as a part of the frozen core, including exchange-correlation core corrections.[16] The electron wave functions were expanded in plane waves with an energy cutoff of 60 Ry, and the Brillouin zone was sampled at special k points according to the Monkhorst-Pack[17] $4\times4\times4$ mesh for the zinc-blende binary compounds BeSe and ZnSe. These conditions permit us to ensure convergence on total energy to less than 10^{-3} Ry.

Bulk $Zn_{1-x}Be_xSe$ crystal studied in this work was modeled using a 64-atom supercell which corresponds to a $2\times2\times2$ conventional cubic cell, adopting the zinc-blende symmetry. Such a system requires many plane waves; furthermore, the combination of the appropriated parameters and powerful computers makes it less difficult. The system made by repeating such a cell may be a representative way to deal with the physical problem of interest. Schematic example of this supercell is displayed in Fig. 1(a). The figure shows one of the C_n^{32} different possible configurations treating the alloy $Zn_{32-n}Be_nSe$ at the composition average $\frac{n}{32}$. From a fundamental point of view, investigating properties of such a system at an averaged composition requires the study of all the possible configurations in order to take into account the disorder in the system. Realizing such a work is impossible because of the enormous analytical time which should be devoted.

One realistic solution is based on the choice of some configurations as well as to give a more representative image of the studied system. In the zinc-blende-like structure, the atoms are tetrahedrally bonded so that each Se atom is surrounded by four cations (Be or Zn) as displayed in Fig. 1(b). In our case, five configurations were used to characterize the alloy; this choice is simply related to the five possible ways to arrange cations around the anion site, so that each of the configurations proposed here favors one of the five different environments of the Se atoms.

In large-supercell calculations (64 atoms), the energy cutoff was chosen to be equal to 40 Ry in order to earn on computing time without compromising accuracy. When comparing total energies issued from a 64-atom (with energy cutoff of 40 Ry and one k point) and 2-atom (energy cutoff

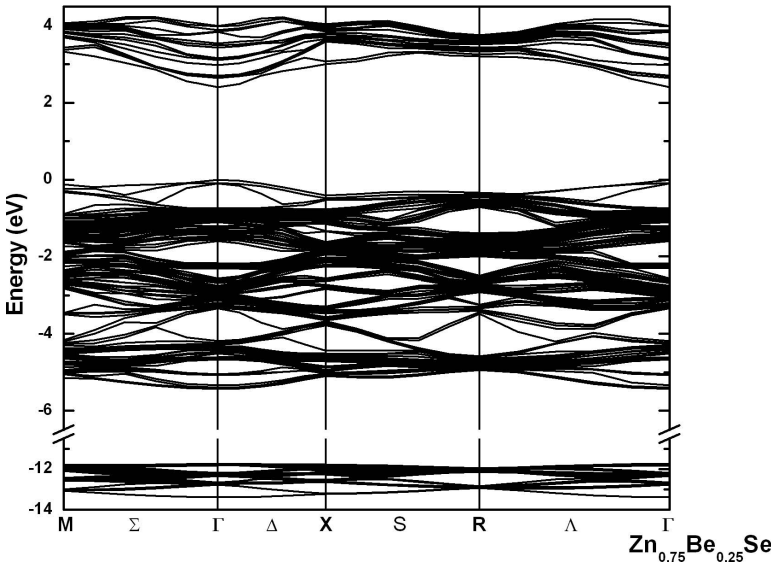

FIG. 2. Energy band structure along the simple cubic high-symmetry directions for $Zn_{0.75}Be_{0.25}Se$.

of 60 Ry and ten special k points) primitive cell calculations adopted for the pure BeSe compound, the total energy difference was about 3 mRy. Convergence on total energy in the self-consistent field was ensured until 10^{-8} Ry. The relaxation of the system was performed according to the "Beeman algorithm for variable cell damped dynamics" for the ionic dynamics[18] and the "damped (Beeman) dynamics of the Parrinello-Rahman extended Lagrangian" for the cell dynamics.[19] The Hellman-Feynman forces acting on each atom were calculated and the structure was relaxed in all directions until these forces were less than 2.6 meV/Å.

The properties of $Zn_{1-x}Be_xSe$ at different beryllium compositions were determined by taking the weighted average of their quantities for the five symmetrically inequivalent configurations treated in the 64-atom supercell. Given a microscopic configuration j, the configuration-averaged properties of $Zn_{1-x}Be_xSe$ are given by

$$P(x) = \sum_{j=0}^{J} x_j P_j, \tag{1}$$

where P_j are the values of the physical properties (total energy, band gap, etc.) for that configuration and x_j the composition-dependent weights determined for an ideal solid solution[20] as

$$x_j = g_j x^j (1-x)^{4-j}. \tag{2}$$

The degeneracy factor g_j is the number of ways of arranging the alloying cations in the cluster. In our case, there are five kinds, $j=0,\ldots,4$ ($J=4$). The degeneracy factors are $g_j=C_j^4=4!/j!(4-j)!$, i.e., $g_0=1$, $g_1=4$, $g_2=6$, $g_3=4$, and $g_4=1$.

III. RESULTS AND DISCUSSION

Before handling the main steps of the present work, let us start with a preliminary study on the bulk materials. We have calculated the structural and electronic properties of ZnSe and BeSe which crystallize in the 2-atom-unit-cell zinc-blende structure. We obtained the lattice parameters of 5.59 and 5.122 Å, respectively. The accuracy of the results is very satisfactory when compared with experimental values of 5.667 and 5.139 Å.[21]

The band structure for the ordered material can be described by the use of a supercell, although it is a more complicated calculation than for the normal cell. Systematic numerical errors can occur when integrating on sampled Brillouin zone of different unit cells (2 and 64 atoms). To overcome such errors, it will be more appropriate to use equivalent set of k points as described by Froyen.[22] One special k point was used for the 64-atom supercell calculation, which was enough for the convergence. Figure 2 shows a representative band structure for $Zn_{1-x}Be_xSe$ at the averaged composition of 25%. We notice that the band structure is plotted with respect to the Brillouin zone of simple cubic 64-atom cell. Since the beryllium substitution breaks the symmetry of the underlying zinc-blende structure, there is no rigorous and well-defined procedure to "unfold" the band structure into the Brillouin zone of the primitive 2-atom zinc-blende unit cell. The high-symmetry points of the primitive ZnSe cell fold into the Γ point of the 64-atom unit cell. Therefore, in the presence of a real symmetry-breaking term, such as produced by beryllium substitution, we can expect interactions between the resulting levels. Figure 3 shows the calculated average band gap for the most important energy transitions ($\Gamma_{15v}\rightarrow\Gamma_{1c}$ and $\Gamma_{15v}\rightarrow X_{1c}$) together with some corresponding experimental data for the $\Gamma\rightarrow\Gamma$ transition obtained by Chauvet *et al.*[4] The calculated band gap for $x=0.25$ is only 2.398 eV, while the experimental one is 3.38 eV.[4] This large error in the band gap is a well-known problem of the LDA, which fails quantitatively in dealing with excited-state properties. The computed values of the direct $\Gamma_{15v}\rightarrow\Gamma_{1c}$ were fitted by polynomial least squares and lead to quadratic term (bowing parameter b) of about 1.08 eV, which compares well with the experimental values of 1.1 eV (Ref. 3) and 0.97 eV.[4] The crossover of direct-indirect gap in the alloy composition variation was found to be at $x=0.36$, which deviates from the experimental value of $x=0.46\pm0.01$.[4] It is worthy to note that the difference found between our calculated band gap and the experimental one

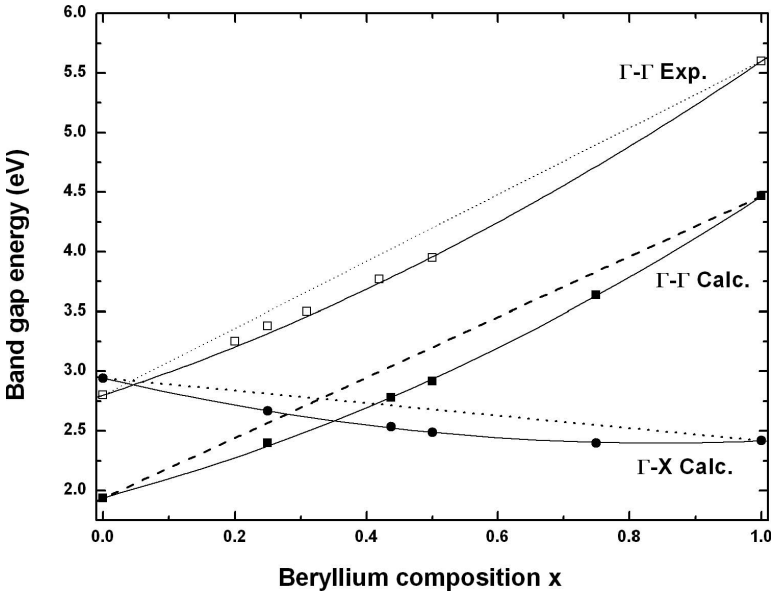

FIG. 3. Variation of the direct band gap (solid squares) and the indirect band gap (solid circles) as a function of beryllium concentration x for $Zn_{1-x}Be_xSe$. Some experimental (Ref. 4) direct band-gap values (open squares) are added for comparison.

does not affect the main goal of the present work, which is about the variation of the band gap and not its absolute value. The calculated variation follows, indeed, the same trends observed experimentally. The error noticed is then relative and not absolute.

A. Optical bowing and its origin

The origin of the widely observed nonlinear dependence of the fundamental band gap on the composition of semiconductor alloys $A_{1-x}B_xC$ was the aim of several studies. Both experimental and theoretical calculations assume a deviation from the linear dependence predicted by the virtual-crystal approximation (VCA).[23] In this approach, the composition dependence of the band gap is described by a second-order polynomial with the quadratic term proportional to the so-called bowing parameter b so that

$$E_g(x) = xE_{BC}(a_{BC}) + (1-x)E_{AC}(a_{AC}) - bx(1-x). \quad (3)$$

In order to better understand the origin of the gap bowing parameter b, Bernard and Zunger[24] decomposed it into three contributions resulting from volume deformation, charge exchange, and structural relaxation.

At a given average composition x, the ternary alloy $Zn_{1-x}Be_xSe$ obeys the formal reaction

$$x\mathrm{BeSe}(a_{\mathrm{BeSe}}) + (1-x)\mathrm{ZnSe}(a_{\mathrm{ZnSe}}) \rightarrow \mathrm{Zn}_{1-x}\mathrm{Be}_x\mathrm{Se}(a_{eq}, u_{eq}), \quad (4)$$

where a_{BeSe} and a_{ZnSe} are the equilibrium lattice constants of the binary compounds BeSe and ZnSe, respectively. a_{eq} and u_{eq} are the equilibrium lattice constant and the equilibrium internal parameter of the alloy at the average composition x. The different contributions to the band-gap bowing b are attributed to the following.

First, volume deformation (b_{VD}) represents changes in the band gaps of the bulk materials ZnSe and BeSe that are compressed and dilated, respectively, from their equilibrium lattice constants to the intermediate alloy one $a_{eq}=a(x)$, according to the following reaction:

$$\mathrm{BeSe}(a_{\mathrm{BeSe}}) + \mathrm{ZnSe}(a_{\mathrm{ZnSe}}) \rightarrow \mathrm{BeSe}(a_{eq}) + \mathrm{ZnSe}(a_{eq}), \quad (5)$$

so that

$$b_{VD} = \frac{E_{\mathrm{BeSe}}(a_{\mathrm{BeSe}}) - E_{\mathrm{BeSe}}(a_{eq})}{1-x} + \frac{E_{\mathrm{ZnSe}}(a_{\mathrm{ZnSe}}) - E_{\mathrm{ZnSe}}(a_{eq})}{x}. \quad (6)$$

Secondly, charge exchange (b_{CE}) represents the change in the band gap upon bringing together the constituents, already prepared at $a_{eq}=a(x)$, without permitting any sublattice relaxation. The formal reaction is

$$x\mathrm{BeSe}(a_{eq}) + (1-x)\mathrm{ZnSe}(a_{eq}) \rightarrow \mathrm{Zn}_{1-x}\mathrm{Be}_x\mathrm{Se}(a_{eq}, u). \quad (7)$$

This term includes charge-transfer effects due to the different bonding behaviors of the two constituents; the contribution of this structural relaxation to the bowing is hence

$$b_{CE} = \frac{E_{\mathrm{BeSe}}(a_{eq})}{1-x} + \frac{E_{\mathrm{ZnSe}}(a_{eq})}{x} - \frac{E_{\mathrm{Zn}_{1-x}\mathrm{Be}_x\mathrm{Se}}(a_{eq}, u)}{x(1-x)}. \quad (8)$$

Finally, structural relaxation (b_{SR}),

$$\mathrm{Zn}_{1-x}\mathrm{Be}_x\mathrm{Se}(a_{eq}, u) \rightarrow \mathrm{Zn}_{1-x}\mathrm{Be}_x\mathrm{Se}(a_{eq}, u_{eq}), \quad (9)$$

represents the change in band gap due to the system relaxation. This term includes atomic-relaxation-induced band mixing,

$$b_{SR} = \frac{E_{\mathrm{Zn}_{1-x}\mathrm{Be}_x\mathrm{Se}}(a_{eq}, u) - E_{\mathrm{Zn}_{1-x}\mathrm{Be}_x\mathrm{Se}}(a_{eq}, u_{eq})}{x(1-x)}. \quad (10)$$

The addition of the three contributions (6), (8), and (10) leads to the total bowing parameter b. The computed bowing coefficients b together with the three different contributions for both the direct and indirect band gaps as a function of the beryllium molar fraction for the $Zn_{1-x}Be_xSe$ alloy are shown

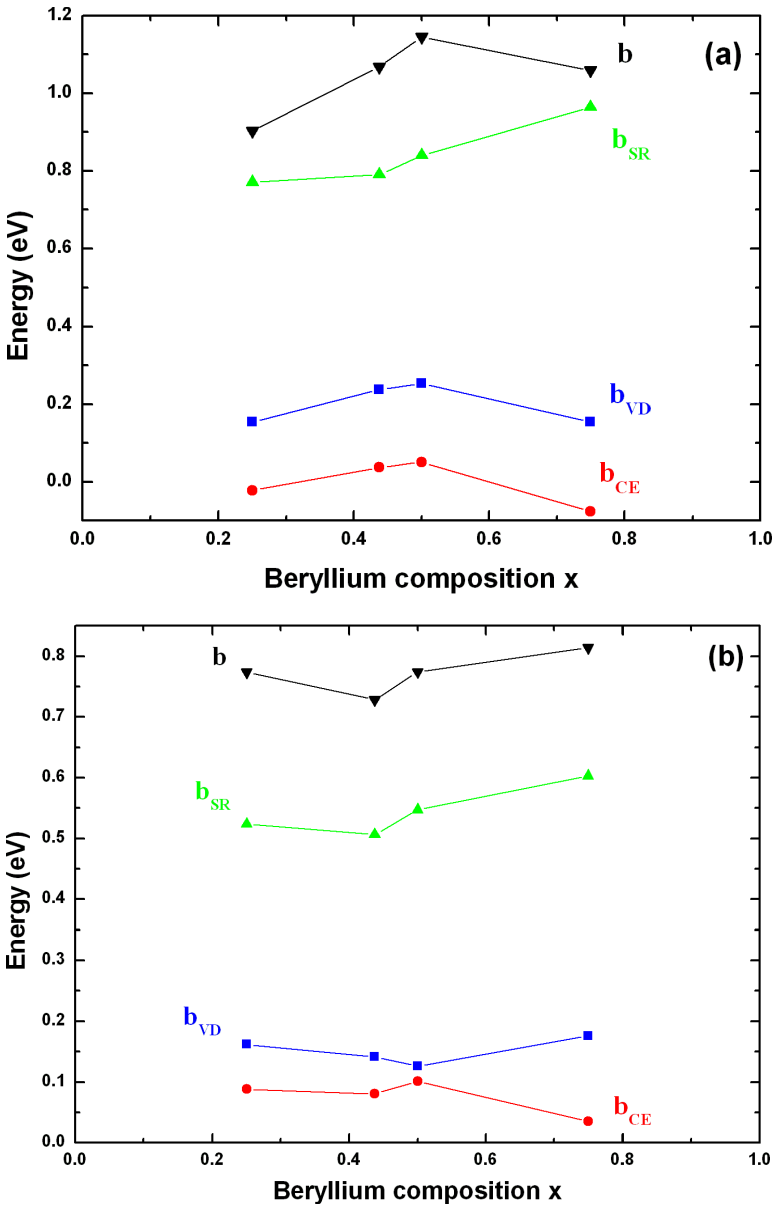

FIG. 4. (Color online) Composition dependence of the average (a) direct $\Gamma \rightarrow \Gamma$ and (b) indirect $\Gamma \rightarrow X$ band-gap bowings (solid down triangles) together with their different contributions; volume deformation b_{VD} (solid squares), charge transfer b_{CE} (solid circles), and structural relaxation b_{SR} (solid down triangles) for $Zn_{1-x}Be_xSe$.

in Figs. 4(a) and 4(b), respectively. We observe the following facts:

(i) Despite the fact of the large mismatch of the lattice constants occurring between the bulk materials (9%), a small volume deformation term (b_{VD}) was registered for $Zn_{1-x}Be_xSe$ system. This can be simply related to the hydrostatic band-gap deformation potentials of the binary alloys.

(ii) The smallest contribution to the gap bowing (b_{CE} sometimes negative) is attributed to the charge transfer. This is related to the electronegativity[25] mismatch, which is very small (0.08) between those of Be (1.57) and Zn atoms (1.65).

(iii) A pronounced and positive structural relaxation contribution (b_{SR}) submerges the two other contributions. This is known to be relative to the large discrepancy between the atomic sizes of the alloyed cations, i.e., covalent radii; the Be ion (covalent radius of 0.90 Å) is much smaller compared with the Zn ion (1.25 Å).[25]

The change in band gap is related to the structural effect and especially to the atomic bond relaxation. Therefore, in order to get better information on this behavior, it is very important to clarify the variation of bond lengths and second-nearest-neighbor distances for the different compositions studied. This will be investigated in the following part.

B. Structural properties

Figure 5(a) shows the averaged values of the computed lattice constant for $Zn_{1-x}Be_xSe$ as a function of the composition x. We found that the configurationally averaged lattice constants fulfill Vegard's law[26] with a small downward deviation bowing of about 0.04 Å. More detailed information on the crystal lattice behavior can be obtained by analyzing the bond lengths $d_{\text{Be-Se}}$ and $d_{\text{Zn-Se}}$ between Be and Se, and Zn and Se, respectively. The results obtained are displayed in

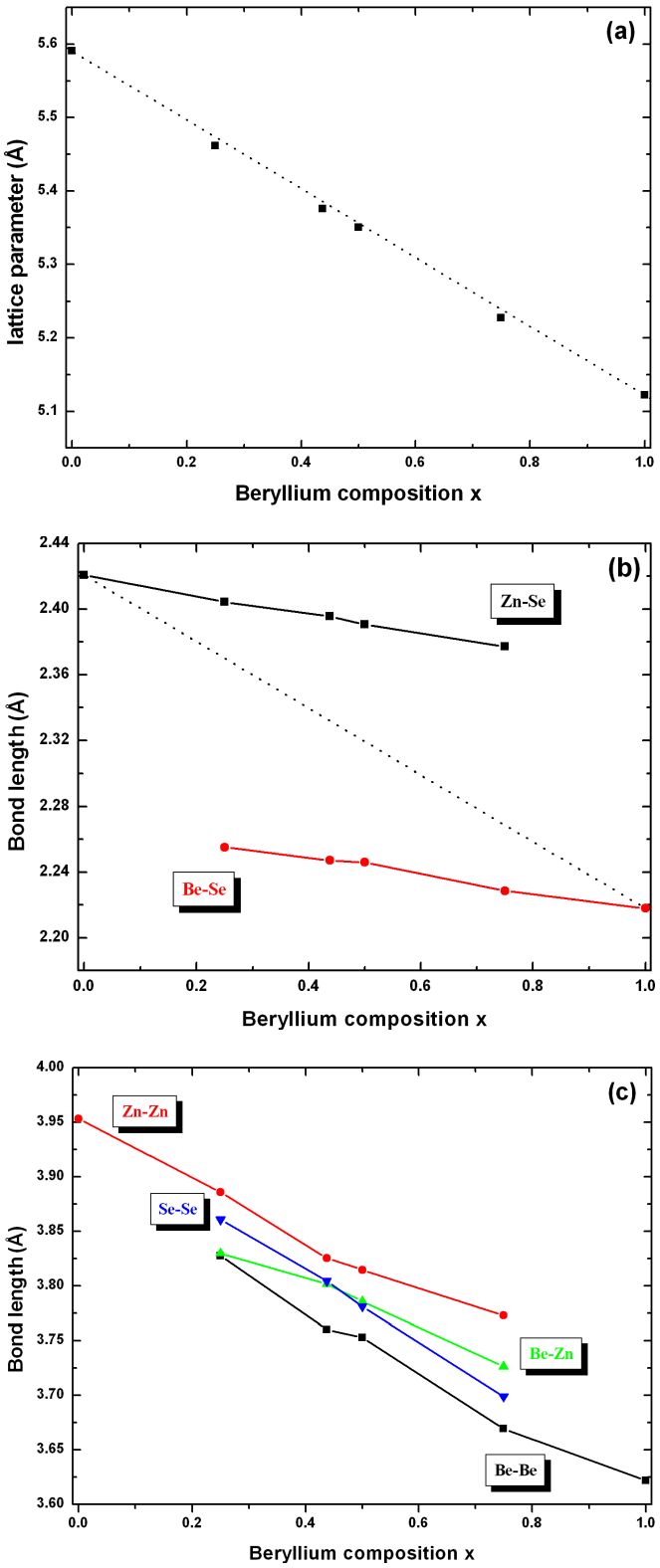

FIG. 5. (Color online) Evolution of the average (a) lattice parameter (solid squares) compared with the VCA (dotted line), (b) the average bond lengths $d_{\text{Be-Se}}$ and $d_{\text{Zn-Se}}$, (c) the second-nearest-neighbor distances 2NN as a function of beryllium concentration in the $Zn_{1-x}Be_xSe$ semiconductor alloy.

Fig. 5(b). The first deduction regarding the first-neighbor distances is a confirmation of the typical behavior of bond lengths in semiconductor alloys. It was found in both theoretical and experimental works that despite the fact that lattice constant follows Vegard's law, the atoms are able to readjust themselves in such a way as to maintain bond lengths similar to those occurring in bulk materials. The variation of the bond lengths is almost evaluated by the average bond-length relaxation parameter

$$\delta(x) = [d_{\text{Zn-Se}}(x) - d_{\text{Be-Se}}(x)]/[d_{\text{Zn-Se}}(0) - d_{\text{Be-Se}}(1)], \tag{11}$$

which ranges from 0 to 1. When $\delta=0$, the lattice is perfectly rigid, so all bonds adjust their lengths to a common value predicted by Vegard's Law, whereas $\delta=1$ would indicate that the lattice is flexible, so every bond adjusts to its natural length observed for the parent binaries; then, we have the Pauling limit.[27] A bimodal distribution of the nearest-neighbor distances was found, as typically observed in other ternary ionic and semiconductor alloys. δ is almost constant and it is predicted from the calculation to be equal to 0.73. Compared with the results obtained by Tsai *et al.*,[8] our calculated lattice constants for binary alloys are in better concordance with experimental ones. Additionally, their calculated alloy equilibrium lattice constant at $x=0.5$ deviates from that determined by Vegard's rule by 4.5% (in our work, the deviation is −0.1%), which is significant and may affect the accuracy of the calculated properties such as bond lengths. This deviation is perhaps due to the insufficiency of the basis set and/or pseudopotential they used. In the investigation on bond lengths, Tsai *et al.* found that the Be-Se bonds for the alloy system ($0.25 \leqslant x \leqslant 0.75$) increase significantly from those of the binary compounds and come near the Zn-Se ones, while in our case, the two types of bonds tend to maintain their values in the corresponding bulk materials (BeSe and ZnSe). They lead to the conclusion that Be-Se bond is more ionic and less rigid than the Zn-Se one. This is in contradiction with the experimental work of Vérié[1] who proposed to introduce beryllium chalcogenides alloys in laser structures and based his proposition on the fact that the higher degree of covalent bonding in Be compounds would increase the resistance of the structures to defect generation and propagation essentially caused by the ionic character of the Zn-Se bonds.

It is also interesting to calculate and to analyze the variation of the second-nearest-neighbor (2*NN*) distances $d_{\text{Be-Be}}$, $d_{\text{Zn-Zn}}$, $d_{\text{Se-Se}}$, and $d_{\text{Be-Zn}}$ as a function of composition. Unfortunately there are no experimental data available for these quantities; our corresponding results are plotted in Fig. 5(c). In contrast to the nearest-neighbor distances, we notice a clear composition dependence of all curves. The 2NN distances exhibits four distinct values: the smallest distance is found for the Be-Be value while the Zn-Zn distance is the largest, and both the Se-Se and Be-Zn lengths are between the extremes.

C. Thermodynamic properties

We investigate in this part the phase stability of $Zn_{1-x}Be_xSe$ solid solution systems based on the regular-

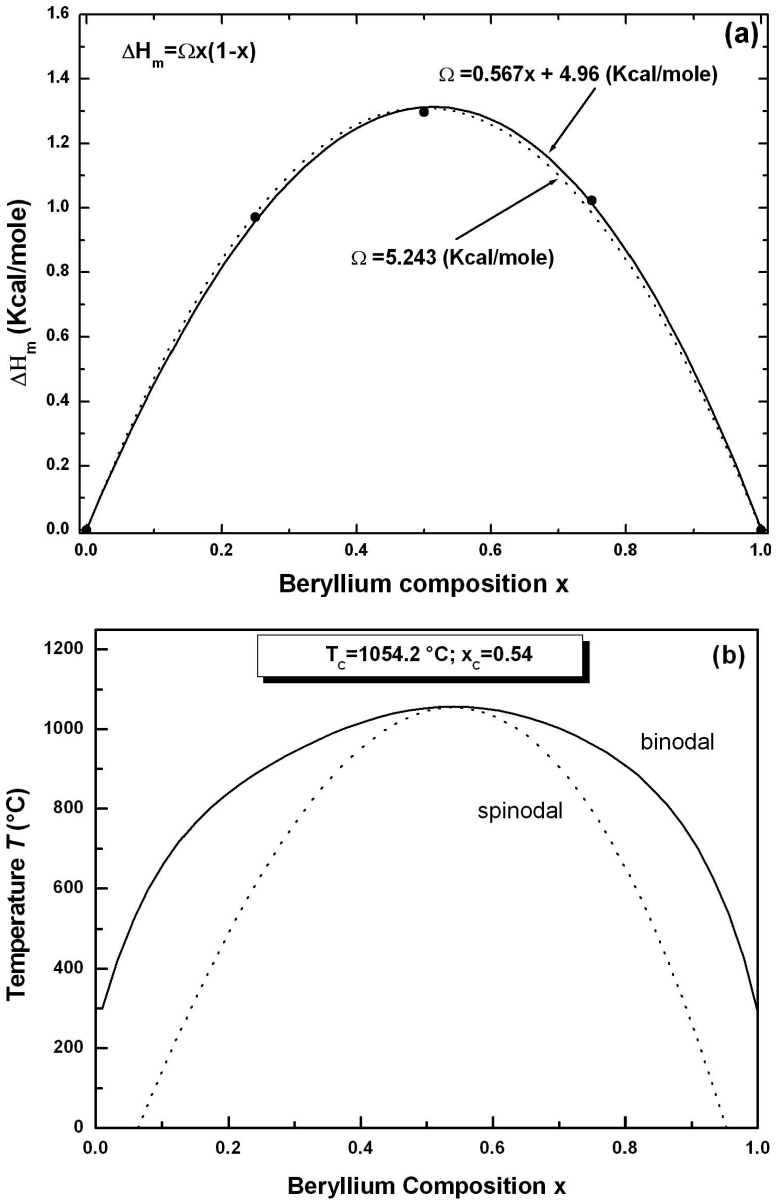

FIG. 6. (a) Enthalpy of mixing ΔH_m and (b) phase diagram calculated using the regular-solution model as a function of beryllium concentration in $Zn_{1-x}Be_xSe$. Solid and dotted curves in (a) present the enthalpy of mixing calculated using the regular-solution model with the x-dependent and x-independent interaction parameters Ω, respectively. The binodal line in the phase diagram (b) is defined by the two branches $x_1=x_1(T)$ and $x_2=x_2(T)$; the spinodal curve is defined by the two branches $x_3=x_3(T)$ and $x_4=x_4(T)$.

solution model[28] as applied to $In_xGa_{1-x}N$ and $In_xAl_{1-x}N$ by Ferhat and Bechstedt.[29] The Gibbs free energy of mixing for the $Zn_{1-x}Be_xSe$ alloy is expressed as

$$\Delta G_m = \Delta H_m - T\Delta S_m, \tag{12}$$

where ΔH_m and ΔS_m are the enthalpy and entropy of mixing, respectively. The mixing enthalpy of $Zn_{1-x}Be_xSe$ alloy can be obtained as the difference in energy between the alloy and the weighted sum of the constituents:

$$\Delta H_m = E_{Zn_{1-x}Be_xSe} - xE_{BeSe} - (1-x)E_{ZnSe}. \tag{13}$$

The resulting averaged formation enthalpies of $Zn_{1-x}Be_xSe$ alloy treated with 64-atom supercell for the compositions $x=0$, 0.25, 0.5, 0.75, and 1 are indicated by the solid circles in Fig. 6(a). ΔH_m has a maximum near $x=0.5$. ΔH_m can also be expressed as

$$\Delta H_m = \Omega x(1-x), \tag{14}$$

where Ω is the interaction parameter which depends on the material. By rewriting expression (14) as $\Omega=\Delta H_m/x(1-x)$, we can calculate, for each x, a value of Ω from the above DFT values of ΔH_m. The only shortcoming we may notice for the regular-solution model for a statistical description of entropy is that the model could be affected by the number of DFT enthalpy values extracted from DFT calculation and, consequently, by the nature of the fit needed. The interaction parameter Ω depending on x is then obtained from a linear fit to the Ω values. Since the entropic contribution to the free-energy difference is always negative, a negative Ω in ΔH_m will lead to a negative ΔG_m over all the composition range and at any temperature. However, if Ω is positive, which is the case in our results, the effect of temperature will be very important at high values. The best fit gives $\Omega=0.567x+4.96$ kcal/mole. The average value of the x-dependent Ω in the range $0\leqslant x\leqslant 1$ is obtained as $\Omega=0.567\times 0.5+4.96$

=5.243 kcal/mole. Next, we calculate ΔH_m expressed by Eq. (14) with $\Omega=0.567x+4.96$ kcal/mole, as drawn by the solid curve in Fig. 6(a). The DFT results of ΔH_m (solid circles) are accurately reproduced by the above ΔH_m curve. Besides, Ω =5.243 kcal/mole independent of x is also used to draw ΔH_m, as shown by the dotted curve in Fig. 6(a). The latter is symmetric around $x=0.5$, while the x-dependent parameter is asymmetric leading to a slight deviation toward the highest x side. The effect of this asymmetry will be pronounced in the phase diagram shown later. The formation energies are all positive as shown in the Fig. 6(a). This implies that the system has strong tendency to segregate in its constituents at low temperature. At high T, disordered configurations are expected to become favored because of the important increase of the entropic term. Our aim here is to determine the behavior of the alloy between such limits.

The alloying entropy ΔS_m is evaluated as $\Delta S_m = -R[x \ln x+(1-x)\ln(1-x)]$, where R is the gas constant. From the variation of ΔG_m as a function of x, we deduce the temperature-composition phase diagram which shows the stable, metastable, and unstable composition regions of a mixed crystal for a given growth temperature. Below a critical temperature T_C, the free energy of mixing, remaining negative, acquires a shape with two minima at two composition points (i.e., binodal points x_1 and x_2) and one maximum. In other way, x_1 and x_2 are the points where common tangent touches the free-energy curve. With the definition of the chemical potential $\mu(x,T)=(\partial/\partial x)G_m(x,T)$, it therefore holds $\mu(x_1,T)=\mu(x_2,T)$. For a composition in the range $0<x<x_1$ or $x_2<x<1$, the solid solution $A_xB_{1-x}C$ phase is thermally stable against decomposition. However, in the composition range of $x_1<x<x_2$, the total Gibbs free energy of the system is lowest if the system remains as a mixture of two immiscible solutions $A_{x_1}B_{1-x_1}C$ and $A_{x_2}B_{1-x_2}C$. The composition region between two binodal points is the miscibility gap. Thermodynamically unstable phases may exist metastably in cases where the decomposition kinetics is slow, combined with rapid quenching. Within the miscibility gap, there also exists two inflection points x_3 and x_4 (spinodal points), where $\partial^2\Delta G_m/\partial x^2=0$. For a composition x between the binodal and spinodal points, the Gibbs free energy increases when the solid solution decomposes locally into a mixture of two compositions in the neighborhood of x. In this sense, there exist local decomposition barriers and the $A_xB_{1-x}C$ phase might exist metastably. Using the interaction parameter $\Omega=0.567x+4.96$ kcal/mole, we quantitatively determine the critical temperature T_C and the stable and/or metastable boundary lines (i.e., the lines linking binodal or spinodal points at various temperatures). In Fig. 6(b), we show the resulting phase diagram of $Zn_{1-x}Be_xSe$. The critical alloy formation temperature occurs at a point where both the first and second derivatives of the free energy are zero, i.e., the plot has no curvature. The miscibility gap disappears at $T_C=1327.36$ K, and it is slightly asymmetric about $x=0.5$ due to the asymmetry of ΔH_m. We obtain a critical composition at $x_C=0.54$. The samples studied in the work of Chauvet *et al.*[4] have been grown on (100) oriented GaAs substrates by solid source molecular-beam epitaxy where the substrate temperature was fixed between 300 and 380 °C. From our phase diagram, more stable semiconductor alloys are likely to form at high temperature, expecting that samples actually used in experiment are well outside equilibrium. These results indicate that $Zn_{1-x}Be_xSe$ alloy is unstable over a wide range of intermediate compositions at normal growth temperatures. This purpose can be supported by the work of Plazaola *et al.*[7] where the $Zn_{1-x}Be_xSe$ crystals were grown from melt (1850 K) using the high-pressure Bridgman method and followed a special procedure in order to obtain better homogeneity of the crystals.

IV. CONCLUSION

We have investigated the composition dependence of the energy gap of $Zn_{1-x}Be_xSe$ ternary alloy using first-principles pseudopotential plane-wave calculations. The semiconductor alloy was modeled using a large supercell of 64 atoms in order to cope with compositional disorder. Nonlinear behavior is observed on the composition dependence of the energy gap, with increasing of beryllium composition. It is found that the shape of the calculated energy band gap and bowing parameter versus Be composition of $Zn_{1-x}Be_xSe$ agree well with the experimental results reported by Chauvet *et al.*[4] accompanied by a down shift caused by the use of LDA approximation. The calculated bowing parameter of $Zn_{1-x}Be_xSe$ corresponds to 1.08 eV, which agrees very well with the experimental values of 1.1 eV (Ref. 3) and 0.97 eV.[4] The investigation of the origin of the band-gap bowing shows that this one is mainly dominated by the contribution provided by the structural effect. In contrast to the lattice parameter, which shows a small deviation from Vegard's law, bond-length distribution exhibits the typical bimodal behavior where each mode deviates faintly from the values they would have in pure compounds. This leads to more realistic behavior compared with those in the preceding theoretical works[8] using the smallest supercell. On the other hand, more important composition dependence is registered for the next-nearest-neighbor distances. Finally, the enthalpy of mixing ΔH_m is calculated in the whole composition range. The calculated ΔH_m is expressed within the regular-solution model $\Delta H_m=\Omega x(1-x)$ using the x-dependent interaction parameter $\Omega=0.567x+4.96$ kcal/mole. The calculated phase diagram indicates a significant phase miscibility gap with a critical temperature estimated at about 1327.36 K. These results indicate that the $Zn_{1-x}Be_xSe$ alloy is unstable over a wide range of intermediate compositions at normal growth temperatures.

*Electronic address: azaoui@polytech-lille.fr

[1] C. Vèrié, International Conference on Semiconductor Heteroepitaxy, Montpellier, France, 4–7 July 1995 (unpublished); Mater. Sci. Eng., B **43**, 60 (1997); Eighth International Conference on II-VI Compounds, Grenoble, France, 25–29 August 1997 (unpublished).

[2] A. Waag, F. Fischer, H. J. Lugauer, Th. Litz, J. Laubender, U. Lunz, U. Zehnder, W. Ossau, T. Gerhardt, M. Möller, and G. Landwehr, J. Appl. Phys. **80**, 792 (1996); A. Waag, F. Fischer, K. Schüll, T. Baron, H.-J. Lugauer, T. Litz, U. Zehnder, W. Ossau, T. Gerhard, M. Keim, and G. Landwehr, Appl. Phys. Lett. **70**, 280 (1997); G. Landwehr, F. Fischer, T. Baron, T. Litz, A. Waag, K. Schüll, H. Lugauer, T. Gerhard, M. Keim, and U. Lunz, Phys. Status Solidi B **202**, 645 (1997); A. Waag, T. Litz, F. Fischer, H.-J. Lugauer, T. Baron, K. Schüll, U. Zehnder, T. Gerhard, U. Lunz, M. Keim, G. Reuscher, and G. Landwehr, J. Cryst. Growth **184/185**, 10 (1998).

[3] K. Wilmers, T. Wethkamp, N. Esser, C. Cobet, W. Richter, V. Wagner, A. Waag, H. Lugauer, F. Fischer, T. Gerhard, M. Keim, and M. Cardona, Phys. Status Solidi B **215**, 15 (1999).

[4] C. Chauvet, E. Tournié, and J.-P. Faurie, Phys. Rev. B **61**, 5332 (2000).

[5] M. W. Cho, J. H. Chang, D. M. Bagnall, K. W. Koh, S. Saeki, K. T. Park, Z. Zhu, K. Higara, and T. Yao, J. Appl. Phys. **85**, 512 (1999).

[6] H. Lee, I.-Y. Kim, J. Powell, D. E. Aspnes, S. Lee, F. Peiris, and J. K. Furdyna, J. Appl. Phys. **88**, 878 (2000).

[7] F. Plazaola, J. Flyktman, K. Saarinen, L. Dobrzynski, F. Firszt, S. Legowski, H. Meczynska, W. Paszkowicz, and H. Reniewicz, J. Appl. Phys. **94**, 1647 (2003).

[8] M.-H. Tsai, F. C. Peiris, S. Lee, and J. K. Furdyna, Phys. Rev. B **65**, 235202 (2002).

[9] A. Zaoui, J. Phys.: Condens. Matter **14**, 4025 (2002); E. Pelucchi, S. Rubini, B. Bonanni, A. Franciosi, A. Zaoui, M. Peressi, A. Baldereschi, D. De Salvador, M. Berti, A. Drigo, and F. Romanato, J. Appl. Phys. **95**, 4184 (2004).

[10] P. Hohenberg and W. Kohn, Phys. Rev. **136**, B864 (1964); W. Kohn and L. J. Sham, Phys. Rev. **140**, A1133 (1965).

[11] S. Baroni, A. Dal Corso, S. de Gironcoli, P. Giannozi, C. Cavazzoni, G. Ballabio, S. Scandolo, G. Chiarotti, P. Marzari, and A. Kokalj, Plane Wave Self Consistent Field, http://www.pwscf.org

[12] D. M. Ceperley and B. J. Alder, Phys. Rev. Lett. **45**, 566 (1980).

[13] J. P. Perdew and A. Zunger, Phys. Rev. B **23**, 5048 (1981).

[14] U. Von Barth and R. Car (unpublished).

[15] G. B. Bachelet, D. R. Hamann, and M. Schlüter, Phys. Rev. B **26**, 4199 (1982).

[16] S. G. Louie, S. Froyen, and M. L. Cohen, Phys. Rev. B **26**, 1738 (1982).

[17] H. J. Monkhorst and J. D. Pack, Phys. Rev. B **13**, 5188 (1976).

[18] D. Beeman, J. Comput. Phys. **20**, 130 (1976).

[19] M. Parrinello and A. Rahman, Phys. Rev. Lett. **45**, 1196 (1980); J. Appl. Phys. **52**, 7182 (1981).

[20] L. K. Teles, J. Furthmüller, L. M. R. Scolfaro, J. R. Leite, and F. Bechstedt, Phys. Rev. B **62**, 2475 (2000).

[21] *Data in Science and Technology. Semiconductors: Others than Group IV Elements and III-V Compounds*, edited by O. Madelung (Springer-Verlag, Berlin, 1992).

[22] S. Froyen, Phys. Rev. B **39**, 3168 (1989).

[23] J. A. Van Vechten and T. K. Bergstresser, Phys. Rev. B **1**, 3351 (1970); R. Hill and D. Richardson, J. Phys. C **4**, L289 (1971).

[24] J. E. Bernard and A. Zunger, Phys. Rev. B **36**, 3199 (1987); G. P. Srivastava, J. L. Martins, and A. Zunger, *ibid.* **31**, 2561 (1985); J. L. Martins and A. Zunger, *ibid.* **32**, 2689 (1985); A. Zunger and J. E. Jaffe, Phys. Rev. Lett. **51**, 662 (1983); J. E. Jaffe and A. Zunger, Phys. Rev. B **29**, 1882 (1984).

[25] W. Sargent, *Table of Periodic Properties of the Elements* (Sargent-Welch Scientific, Skokie, IL, 1980).

[26] L. Vegard, Z. Phys. **5**, 17 (1921).

[27] L. Pauling, *The Nature of the Chemical Bond* (Cornell University Press, Ithaca, NY, 1967).

[28] For example, R. A. Swalin, *Thermodynamics of Solids* (Wiley, New York, 1961).

[29] M. Ferhat and F. Bechstedt, Phys. Rev. B **65**, 075213 (2002).